Far-field resonance fluorescence from a dipole-interacting laser-driven cold atomic gas

2017 J. Phys. B: At. Mol. Opt. Phys. 50 014004

(http://iopscience.iop.org/0953-4075/50/1/014004)

OPEN ACCESS
IOP Publishing
Journal of Physics B: Atomic, Molecular and Optical Physics
J. Phys. B: At. Mol. Opt. Phys. **50** (2017) 014004 (7pp)
doi:10.1088/1361-6455/50/1/014004

Far-field resonance fluorescence from a dipole-interacting laser-driven cold atomic gas

Ryan Jones[1,2], **Reece Saint**[1] **and Beatriz Olmos**[1,2,3]

[1] School of Physics and Astronomy, The University of Nottingham, Nottingham, NG7 2RD, UK
[2] Centre for the Mathematics and Theoretical Physics of Quantum Non-equilibrium Systems, The University of Nottingham, Nottingham, NG7 2RD, UK

E-mail: beatriz.olmos-sanchez@nottingham.ac.uk

Received 28 June 2016, revised 18 August 2016
Accepted for publication 13 September 2016
Published 6 December 2016

Abstract

We analyze the temporal response of the fluorescence light that is emitted from a dense gas of cold atoms driven by a laser. When the average interatomic distance is comparable to the wavelength of the photons scattered by the atoms, the system exhibits strong dipolar interactions and collective dissipation. We solve the exact dynamics of small systems with different geometries and show how these collective features are manifest in the scattered light properties such as the photon emission rate, the power spectrum and the second-order correlation function. By calculating these quantities beyond the weak (linear) driving limit, we make progress in understanding the signatures of collective behavior in these many-body systems. Furthermore, we shed light on the role of disorder and averaging on the resonance fluorescence, of direct relevance for recent experimental efforts that aim at the exploration of many-body effects in dipole–dipole interacting gases of atoms.

Keywords: open quantum systems, superradiance, fluorescence

(Some figures may appear in colour only in the online journal)

1. Introduction

Strong dipole–dipole interactions are induced in a gas of emitters due to virtual exchange of photons when the average distance between the emitters is comparable to the wavelength associated to the emitted photons. Moreover, in these gases the radiation properties are modified due to the emergence of collective super and subradiant emission modes. The unique character of such a system was studied for the first time decades ago in the seminal papers by Dicke, Lehmberg and Agarwal among others [1–3].

The unprecedented experimental control available nowadays over the trapping and interactions in ultracold atomic gases [4] has sparked a renewed interest in the investigation of these fundamentally collective effects. Experimental measurements of features such as the collective Lamb shift [5–7], suppression of light scattering and modified spectra from dense samples of atoms [8–13] and observation of super and subradiance [5, 14–16] have been recently realized. Theoretical works so far have been constrained to the study of the limit of very weak driving [17–29], small systems of two or three atoms [30–35] or dilute gases under strong driving conditions [36]. These, however, do not provide a complete picture and leave a number of unanswered questions: (A) How does the presence of strong laser driving affect the signatures of cooperativity detectable in the fluorescence

[3] This article belongs to the special issue: emerging leaders, which features invited work from the best early-career researchers working within the scope of JPhysB. This project is part of the *Journal of Physics* series' 50th anniversary celebrations in 2017. Beatriz Olmos was selected by the Editorial Board of JPhysB as an Emerging Leader.

photons scattered from a dipolar system? (B) Photon emission rate and excitation number have a one-to-one relation when the emitters are independent that is broken when the dissipation becomes collective. What can we learn from this dichotomy? (C) How does the specific external configuration of the atoms affect the previous results? E.g., how does the average over many configurations differ from a single shot, and, are there any differences expected to arise in experimental setups with atoms in ordered (e.g. optical lattices) configurations?

We tackle the above questions in this paper by performing a detailed theoretical analysis of the excitation number, photon emission rate, power spectrum and second-order correlations of the far-field fluorescence from a resonantly driven gas of two-level atoms in the stationary state. We perform this task by solving numerically for the first time the *exact* dynamics of small atomic systems of up to 7 atoms for a broad range of values of the laser driving.

We first focus our efforts on analyzing the emission properties of a three-dimensional (3D) disordered gas, where the positions of the atoms are chosen randomly in 1000 different realizations and the results are then averaged. The results here remain largely independent of the system size and thus give insights into the behavior of larger systems and makes them of direct relevance to current experimental efforts that study the effect of dipole–dipole interactions and collective dissipation in the optical response of a cold atomic system in the absence of inhomogeneous broadening [8–10, 12, 13, 16]. Moreover, in an attempt to illustrate the role of ordered configurations in the emission properties of the system, we have also considered a one-dimensional (1D) lattice of atoms (see figure 1). While some characteristics remain unchanged with respect to the disordered 3D gas, such as the suppression of emission at high densities, finite size effects play an important role here, e.g. in the photon emission correlations.

2. The system

We consider an ensemble of N atoms either confined in an optical lattice or in a disordered gas (see figure 1). All atoms are initially assumed to be in the electronic ground state, $|g\rangle$. An external laser field linearly polarized along the z-axis is then applied to couple resonantly the two internal states $|g\rangle$ and $|e\rangle$. The average interatomic distance between neighboring atoms, a, is here generally considered to be shorter than the transition wavelength λ (see figure 1). As a consequence, strong long-range interactions are induced among the atoms and the photon emission acquires a marked collective character [1–3].

The dynamics of the ensemble is described by the master equation

$$\dot{\rho} = -\frac{\mathrm{i}}{\hbar}[H, \rho] + \mathcal{D}(\rho), \tag{1}$$

where ρ is the atomic density matrix. The many-body

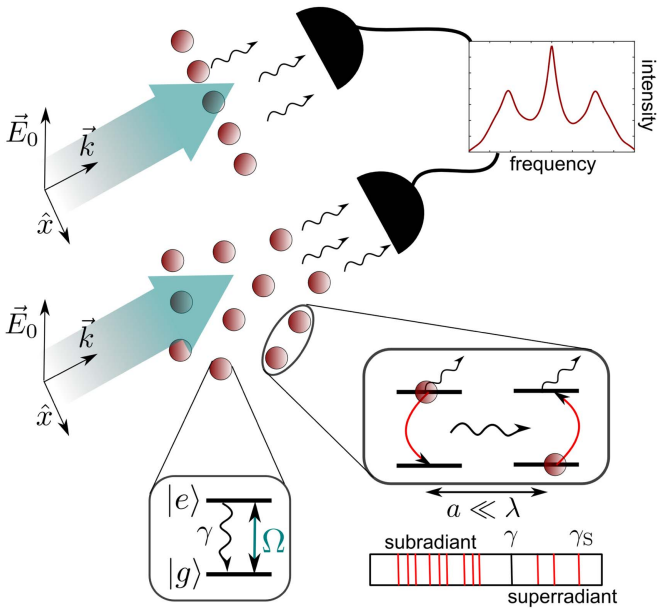

Figure 1. An ensemble of N two-level atoms (a one-dimensional chain along the x-axis or a 3D disordered gas) is illuminated uniformly by a laser field polarized along the z-axis (momentum in the y-direction), which resonantly couples the atomic $|g\rangle - |e\rangle$ transition with Rabi frequency Ω. The virtual exchange of photons gives rise to long-range exchange interactions and collective dissipation conformed by modes with some decay rates larger than the single atom one γ (superradiant) and some smaller than γ (subradiant). These features are most prominent when the interatomic distance a between the atoms is much smaller than the wavelength of the transition λ. We calculate the intensity and spectrum of the resonance fluorescence of the emitted radiation.

Hamiltonian H is expressed as

$$H = \hbar \sum_{\alpha=1}^{N} \Omega(b_\alpha^\dagger \mathrm{e}^{\mathrm{i}\mathbf{k}\cdot\mathbf{r}_\alpha} + b_\alpha \mathrm{e}^{-\mathrm{i}\mathbf{k}\cdot\mathbf{r}_\alpha}) + \hbar \sum_{\alpha\neq\beta} V_{\alpha\beta} b_\alpha^\dagger b_\beta,$$

where we have defined the atomic transition operator $b_\alpha \equiv |g\rangle_\alpha\langle e|$ for the αth atom. The atom-laser coupling strength is given by the Rabi frequency $\Omega = dE_0/(2\hbar)$ with E_0 being the amplitude of the external homogeneous laser field and d the transition dipole moment between the two internal states $|g\rangle$ and $|e\rangle$. The driving field wavevector is denoted by $\mathbf{k} = k\hat{\mathbf{y}}$ (see figure 1) and the spatial position of the αth atom is $\mathbf{r}_\alpha$. Note that we consider the whole system uniformly and simultaneously illuminated by the laser. Hence, propagation effects such as screening from the first atoms of the gas do not lie within the scope of this paper.

The second term of this Hamiltonian represents a coherent exchange interaction between the atoms in the system, which has long-range character. In particular, the interaction between the αth and βth atoms separated by $\mathbf{r}_{\alpha\beta} = r_{\alpha\beta}\hat{\mathbf{r}}_{\alpha\beta}$ is characterized by the coefficient

$$V_{\alpha\beta} = \frac{3\gamma}{4}\left[y_0(\kappa_{\alpha\beta}) - \frac{y_1(\kappa_{\alpha\beta})}{\kappa_{\alpha\beta}} + y_2(\kappa_{\alpha\beta})(\hat{\mathbf{d}}\cdot\hat{\mathbf{r}}_{\alpha\beta})^2\right],$$

where $y_n(x)$ denotes the spherical Bessel function of the second kind, γ the single atom spontaneous decay rate from the excited state and $\hat{\mathbf{d}}$ the direction of the transition dipole

moment. We have also introduced the reduced length $\kappa_{\alpha\beta} = 2\pi r_{\alpha\beta}/\lambda$. For short distances between the atoms, the form of the interaction is close to $1/\kappa^3_{\alpha\beta}$, while it decays as $1/\kappa_{\alpha\beta}$ for long distances, making the collective effects persist even in relatively dilute systems [36].

The second term of equation (1) describes the spontaneous emission of photons from the system and takes the form

$$\mathcal{D}(\rho) = \sum_{\alpha,\beta}\Gamma_{\alpha\beta}\left(b_\alpha \rho b_\beta^\dagger - \frac{1}{2}\{b_\alpha^\dagger b_\beta,\, \rho\}\right),$$

where

$$\Gamma_{\alpha\beta} = \frac{3\gamma}{2}\left[j_0(\kappa_{\alpha\beta}) - \frac{j_1(\kappa_{\alpha\beta})}{\kappa_{\alpha\beta}} + j_2(\kappa_{\alpha\beta})(\hat{\mathbf{d}}\cdot\hat{\mathbf{r}}_{\alpha\beta})^2\right].$$

Here, $j_n(x)$ denotes the spherical Bessel function of the first kind. We are interested in the regime where the distance between the atoms is smaller or comparable to λ, i.e. $\kappa_{\alpha\beta} \leqslant 1$. One can unravel the collective character of the dissipation in this regime by diagonalizing this coefficient matrix as $\Gamma_{\alpha\beta} = \sum_m M^\dagger_{\alpha m}\gamma_m M_{m\beta}$. We can then rewrite the dissipation term in diagonal form as

$$\mathcal{D}(\rho) = \sum_{m=1}^{N}\gamma_m\left(J_m \rho J_m^\dagger - \frac{1}{2}\{J_m^\dagger J_m,\, \rho\}\right),$$

where it is easy to identify

$$J_m = \sum_\alpha M_{m\alpha} b_\alpha$$

as an operator associated to the emission of a photon and γ_m the rate at which such an emission takes place. Note here that the operators J_m do not represent independent modes, as they are conformed by superpositions of spin operators and in general $[J_m, J_n^\dagger] \neq 0\ \forall\, m \neq n$. However, the introduction of these operators is instructive as their structure dictates to which extent the emission and the atomic excitation are coupled (as it will be discussed in the next section) and it allows for an intuitive understanding of the collective character of the emission: In a gas where all $\kappa_{\alpha\beta} \gg 1$, the matrix $\Gamma_{\alpha\beta}$ is approximately diagonal ($M_{m\alpha} \approx \delta_{m\alpha}$). Hence, $J_m \approx b_m$ and $\gamma_m \approx \gamma$ for all $m = 1 \ldots N$, i.e. the photon emissions occur independently from each atom. However, as $\kappa_{\alpha\beta}$ decreases, $M_{m\alpha}$ differs from $\delta_{m\alpha}$ and thus the emission operators J_m become a superposition of several b_α. Hence, here we can understand the incoherent emission of photons as occurring through collective *superradiant* processes with $\gamma_m > \gamma$ and *subradiant* ones with $\gamma_m < \gamma$. The fraction of superradiant emission operators stays almost constant and small as the system size N is increased. In the following, we will denote the largest collective decay rate γ_S (see figure 1).

In the following sections, we proceed to calculate numerically several properties of the system described above and the light scattered from it in the stationary state. In order to obtain this stationary state, we calculate numerically the time evolution of the system by solving exactly the master equation (1) that describes its dynamics. As no further approximations are being made and with the dimension of the density matrix ρ being $2^N \times 2^N$, this problem involves the solution of 2^{2N} coupled differential equations with, in general, 2^{4N} coefficients. This complexity sets a hard constraint on the system sizes we can deal with. In particular, $N = 7$ is the largest system we treat. Moreover, in the 3D disordered gas we need to repeat the numerical experiment 1000 times, which increases dramatically the computation time. Hence, we only show the results in this case for a smaller system size, $N = 5$.

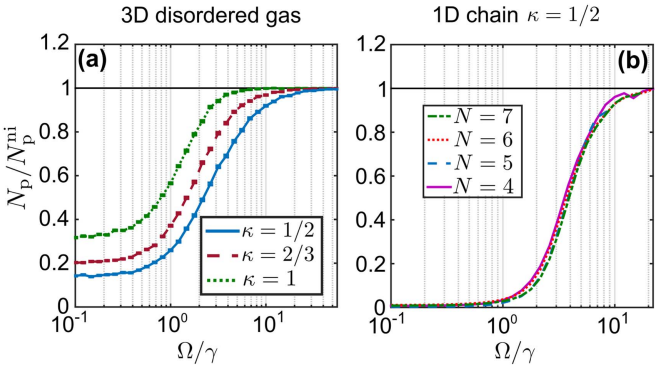

Figure 2. Photon emission rate in a dense gas N_p is suppressed with respect to a non-interacting one N_p^{ni} for a large range of values of the driving Ω. N_p/N_p^{ni} is shown (a) in a 3D disordered gas with $N = 5$ and $\kappa = 1$, $2/3$ and $1/2$ and (b) in a 1D chain with $\kappa = 1/2$ and $N = 4$, 5, 6 and 7.

3. Photon emission in ordered and disordered gases

Our aim is to explore the signatures of collective behavior in the light scattered from the system in the stationary state by solving equation (1) numerically. One of these signatures, which has been observed in experiments such as [8] under weak driving conditions ($\Omega/\gamma \ll 1$), is the strong suppression of the photon emission rate. One can obtain this quantity in terms of the emission operators and rates discussed above (see, e.g. equation (40) in [2]) as

$$N_p = \sum_{m=1}^{N}\gamma_m \langle J_m^\dagger J_m\rangle_{ss}, \qquad (2)$$

where $\langle\cdot\rangle_{ss}$ denotes the expectation value in the stationary state. Note that this definition is equivalent to the integral over all observation directions of the emission rate into a direction $\hat{\mathbf{r}}$, which is proportional to $\langle \mathbf{E}(\mathbf{r}, t)\cdot\mathbf{E}^\dagger(\mathbf{r}, t)\rangle_{ss}$, where $\mathbf{E}(\mathbf{r}, t)$ denotes the negative-frequency part of the electric field operator in the far-zone approximation and in the Heisenberg picture, which is given by [31, 37]

$$\mathbf{E}(\mathbf{r}, t) = \frac{\omega_a^2}{4\pi c^2}\sum_{\alpha=1}^{N}\frac{\hat{\mathbf{r}}\times\hat{\mathbf{r}}\times\mathbf{d}}{|\mathbf{r}-\mathbf{r}_\alpha|}b_\alpha^\dagger\left(t - \frac{|\mathbf{r}-\mathbf{r}_\alpha|}{c}\right),$$

where $\omega_a = 2\pi c/\lambda$.

In figures 2(a) and (b) we compare the results of the emission rate with the non-interacting limit N_p^{ni} for a 3D disordered gas (average results of 1000 realizations) and a 1D chain along the x-axis (perpendicular to the laser momentum, see figure 1), respectively. We characterize the collective behavior in the system by the parameter $\kappa = 2\pi a/\lambda$, where a

represents the average distance between each atom and the one closest to it in the 3D disordered case and the lattice constant in the 1D chain. In both cases we observe strong suppression of the emission for small values of Ω/γ. This suppression, although less pronounced, is still present for values of the driving Ω comparable to the single atom decay rate γ. For large enough Ω/γ, the suppression disappears and $N_{\rm p}/N_{\rm p}^{\rm ni} \to 1$.

In the 3D disordered system the behavior of $N_{\rm p}/N_{\rm p}^{\rm ni}$ as a function of Ω/γ remains unchanged for all system sizes explored (note, only one size is shown in figure 2(a)), which indicates that insights on the behavior of larger systems can be indeed extracted from these results. The lower the value of κ the more pronounced the suppression is for all values of Ω. We also calculate the ratio $N_{\rm p}/N_{\rm p}^{\rm ni}$ in the 1D chain with $\kappa = 1/2$ (figure 2(b)). While the suppression is more pronounced in this case, we observe a very similar qualitative behavior to the disordered case. Again, only minor differences exist between the results for $N = 4 - 7$ atoms (shown in this case in the figure). The results seem to indicate that the emission suppression is a very robust feature of these interacting systems with collective dissipation that survives the addition of finite driving and that does not depend on the specific spatial arrangement of the atoms.

The introduction of the collective emission operators J_m allows us to write explicitly the relation between the emission rate (2) and the number of excitations in the stationary state $N_{\rm e}$ as

$$N_{\rm p} = \sum_{\alpha=1}^{N} \gamma \langle b_\alpha^\dagger b_\alpha \rangle_{\rm ss} + \sum_{\alpha \neq \beta} \Gamma_{\alpha\beta} \langle b_\alpha^\dagger b_\beta \rangle_{\rm ss} = \gamma N_{\rm e} + \sum_{\alpha \neq \beta} \Gamma_{\alpha\beta} \langle b_\alpha^\dagger b_\beta \rangle_{\rm ss}.$$

As we discussed above, in a non-interacting gas the emission operators coincide with the atomic transition ones and hence, for all $\alpha \neq \beta$, $\Gamma_{\alpha\beta} = 0$. Thus, here the emission rate (2) is equivalent to the number of excitations in the stationary state multiplied by the single atom decay rate γ. This relation, however, does not hold in general as the dissipation acquires a collective character [38, 39] and, moreover, the difference between both quantities actually can give us a measure of the coherences of the stationary state of the system $\langle b_\alpha^\dagger b_\beta \rangle_{\rm ss}$.

In figures 3(a) and (b) $N_{\rm p} - \gamma N_{\rm e}$ is shown as a function of Ω/γ. We observe that both in the case of a 3D disordered gas and in a 1D chain the coherences differ from zero except in the limits of very weak and very strong driving: In the very weak driving limit ($\Omega \ll \gamma$) the number of excitations in the stationary state is very small and thus it follows from the Cauchy–Schwarz inequality that the coherences must also be very small. In the limit of very strong driving ($\Omega \gg \gamma$) the dipole–dipole interactions (whose strength is proportional to γ) are much smaller than the driving. Hence, in the stationary state the coherences created by these exchange interactions are also very small, i.e. $N_{\rm p}^{\Omega \gg \gamma} \approx \gamma N_{\rm e}^{\Omega \gg \gamma} = \gamma N/2$.

For intermediate values of the driving, however, we can see that the results differ between the 1D ordered configuration, where the coherences are almost always negative, and the average over many in the 3D random gas, where they change sign at intermediate values of the driving. This change could be attributed to the different geometry of the two systems (1D versus 3D). Note (figure 3(a)) that in the 3D disordered gas the average of $N_{\rm p} - \gamma N_{\rm e}$ is again largely independent of the system size. However, the values for each independent configuration fluctuate notably from one to another, represented by large error bars. Finally, in figure 3(b) (1D chain) one can observe that, while finite size effects are appreciable, the qualitative features of $N_{\rm p} - \gamma N_{\rm e}$ remain similar.

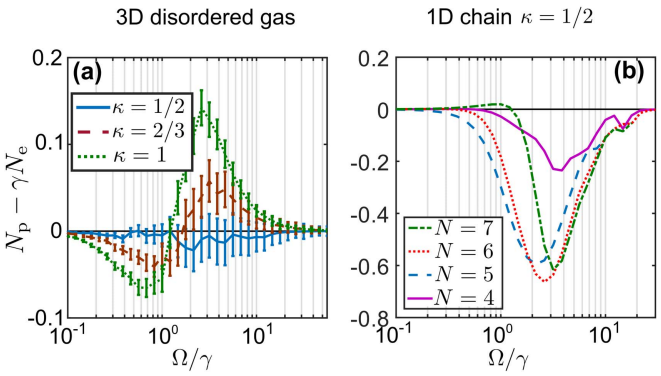

Figure 3. The emission rate is equal to the excitation number $N_{\rm e}$ times γ in the non-interacting limit. We show $N_{\rm p} - \gamma N_{\rm e}$ in a dense gas as a function of Ω/γ (a) in a 3D disordered gas with $N = 5$ and (b) a 1D chain with $\kappa = 1/2$.

4. Resonance fluorescence

Further signatures of collective behavior can be found in the spectral properties of the light emitted by the system. Here, we calculate numerically the power spectrum of the light emitted by the system in the forward direction $\mathbf{r} = r\hat{\mathbf{y}}$. The power spectrum is defined in terms of the electric field operator as

$$S(\mathbf{r}, \omega) = \frac{1}{\pi} {\rm Re} \int_0^\infty {\rm e}^{{\rm i}\omega\tau} \langle \mathbf{E}(\mathbf{r}, t) \cdot \mathbf{E}^\dagger(\mathbf{r}, t + \tau) \rangle_{\rm ss} \, {\rm d}\tau.$$

The results of the numerical calculation of the power spectrum in the far field are shown in figure 4 with $\kappa = 1/2$ and for two values of $\Omega/\gamma = 0.1$ and 10, representative of low and strong driving, respectively. We once again compute the results for a 1D chain and a 3D disordered gas (the latter averaged over 1000 realizations). We also show for comparison the spectrum from a non-interacting gas, which in the low driving regime is formed by a single peak with width smaller than γ and in the strong driving one by a so-called Mollow triplet [37, 40].

When the system is strongly driven (figures 4(a) and (b)), the two cases show similar features: the interactions in the system lead to a broadening of the three peaks of the Mollow triplet. In order to explain this result let us write the master

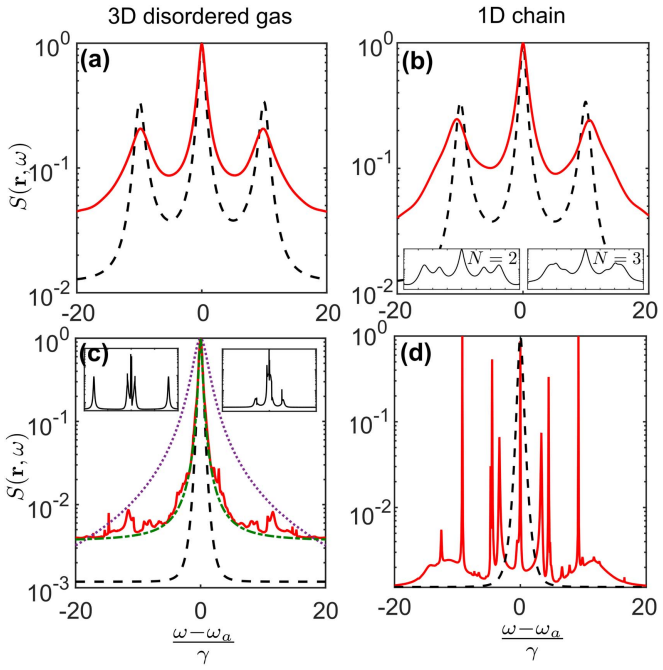

Figure 4. Power spectrum for a non-interacting (dashed black lines) and interacting (red solid lines) gas with $\kappa = 1/2$. (a) and (b) Show broadening of the Mollow triplet in the case of strong driving ($\Omega = 10\gamma$) for a disordered 3D gas of $N = 5$ atoms and 1D chain of $N = 7$ atoms, respectively. The insets show the results for $N = 2$ and 3 for a 1D chain. (c) When $\Omega = 0.1\gamma$ for a disordered 3D gas, the individual realizations give rise to spectra (insets) very different from the average one, which can be fitted with a Lorentzian (green dashed–dotted line). For comparison, a Lorentzian with width γ_S is also shown (purple dotted line). (d) Spectrum of a 1D chain of $N = 7$ atoms for $\Omega = 0.1\gamma$.

equation (1) in terms of the emission operators J_m as

$$\dot{\rho} = \sum_{m=1}^{N} -\mathrm{i}\left[\Omega_m (J_m^\dagger + J_m) + \sum_{n=1}^{N} V'_{mn} J_m^\dagger J_n,\ \rho\right] + \gamma_m\left(J_m \rho J_m^\dagger - \frac{1}{2}\{J_m^\dagger J_m,\ \rho\}\right),$$

where $\Omega_m = \Omega\sum_\alpha M_{m\alpha} e^{i\mathbf{k}\cdot\mathbf{r}_\alpha}$ and $V'_{mn} = \sum_{\alpha,\beta} M_{m\alpha} V_{\alpha\beta} M^\dagger_{\beta n}$. In the strong driving limit ($\Omega \gg \gamma$) the interactions between different modes V'_{mn} for $m \neq n$ are—approximately—negligible compared to the driving strength. After neglecting those cross terms the resulting equation is a sum of N terms with the same form, one for each mode J_m. However, as each $\Omega_m \gg \gamma_m \approx V'_{mm}$, we can approximately assume that each mode gives rise to a Mollow triplet-like contribution to the spectrum, whose sum is the resulting broadened spectrum. While this last step is an approximation given that the emission modes are not strictly independent, this explanation is further substantiated by the spectra for smaller system sizes shown in the insets of figure 4(b), where the 'individual' Mollow triplets are apparent.

On the other hand, in the low driving case the differences between a single realization and many are clear. In each individual realization in the 3D disordered case (insets in figure 4(c)) and the 1D chain (figure 4(d)) we can observe a large number of peaks with width larger (smaller) than the single atom one, corresponding to 'superradiant' ('subradiant') states. The averaging process over all these configurations, where the positions and amplitudes of the subradiant and superradiant peaks are shifted in every run gives as a result a single Lorentzian-like peak broader than the non-interacting one. Note that this width is noticeably smaller than the decay rate of the most superradiant mode γ_S, contrary to what was speculated in [8]. Finally, note that no shifts of the central feature are observed [12, 13].

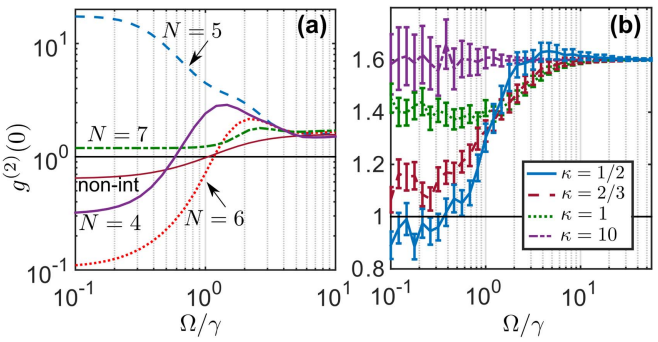

Figure 5. Second-order correlation function $g^{(2)}(\tau = 0)$ as a function of Ω/γ. (a) Data for a 1D chain with size $N = 4$, 5, 6 and 7 with $\kappa = 1/2$. (b) Data for a system of $N = 5$ atoms in a 3D disordered gas for different values of κ. The non-interacting limit ($\kappa = 10$) for $N = 5$ is shown in both panels for comparison.

5. Second order correlation function

The second-order correlation of the resonance fluorescence from different light sources has been widely investigated: It has been established that a thermal source emits photons in bunches, while antibunched photon emission is only seen in quantum light [37, 41–43]. We investigate here the second-order correlation function of the scattered light in our system, defined as

$$g^{(2)}(\tau) = \frac{\langle \mathbf{E}(\mathbf{r},t)\mathbf{E}(\mathbf{r},t+\tau)\mathbf{E}^\dagger(\mathbf{r},t+\tau)\mathbf{E}^\dagger(\mathbf{r},t)\rangle}{\langle I(\mathbf{r},t)\rangle\langle I(\mathbf{r},t+\tau)\rangle}, \quad (3)$$

where $I(\mathbf{r},t) = \mathbf{E}(\mathbf{r},t)\mathbf{E}^\dagger(\mathbf{r},t)$. Equation (3) yields the probability of detecting a photon at time $t+\tau$ given that one was detected at time t divided by the probability of uncorrelated detection. As the atomic ensemble is in the stationary state, $t \to \infty$, the intensity correlation depends only on the time delay τ.

Figure 5 displays data of the second-order correlation $g^{(2)}(\tau)$ at $\tau = 0$ in a dense gas (again the direction of obervation is fixed to be $\hat{\mathbf{y}}$), where we show for comparison the results for $\kappa = 10$ (close to the non-interacting situation). Once more, in the limit of strong driving all curves tend to the same value $g^{(2)}(0) = 2(1 - 1/N)$ [44]. Away from this limit, the results for a single realization in a specific geometry (1D chain, figure 5(a)) show obvious changes as we change the system size. These kind of odd–even effects in the second order correlation functions in a 1D chain were already found in similar studies [45, 46], where superbunching (correlation values larger than the classical upper limit, which we also find

in our system) was reported. These effects disappear in the 3D disordered gas (figure 5(b)), where due to the averaging over many different configurations $g^{(2)}(0)$ is largely independent of the system size. We observe that here the signature of the collective behavior in the system is a reduction of $g^{(2)}(0)$ with respect to the non-interacting case for low values of Ω/γ, with even antibunching being reached in the case of $\kappa = 1/2$ and weak driving.

6. Conclusions and outlook

To conclude, let us return to the three questions posed in the introduction of the paper. (A) In the weak driving regime we observe suppression of photon emission rate, which, albeit less pronounced, is still present for a large range of values of the driving. Moreover, clear signatures of the strong interactions and collective dissipation in this regime are visible in the broadening of the spectrum (Mollow triplet). (B) The fact that there is no simple one-to-one relation between the excitation density and the photon emission intensity can be observed in this system as a signature of collective behavior and can give us information on the coherences of the stationary state. (C) Finally, we show that in general the averaged properties of the scattered light in a disordered gas are qualitatively different from the ones obtained in a single realization. The reason can be found in the averaging process, that washes out the specific features of each single realization.

In this paper we have focused on the effects on the radiation from a dense sample that arise exclusively from the induced many-body exchange interaction and collective dissipation and have left out other effects. For example, throughout this paper, the atoms have been considered to be 'frozen' in their external positions. A natural extension of this work will entail analyzing the effects of external atomic motion, very relevant in some experimentally situations such as a thermal atomic gas [11, 12]. Moreover, as the optical depth gets higher the effect of intensity screening from the first atoms of the system will become important. These effects will be less relevant in a dense ordered gas, where we have shown that the interaction effects are most pronounced. Experiments that explore the dense regime in these ordered configurations have not been performed yet. Strontium atoms possess a very long wavelength transition between low-lying levels and can be trapped in lattices with lattice constant on the order of a few hundred nm [24]. Hence, they represent an ideal platform for the observation of collective effects in dense atomic gases.

Finally, let us remark that we have assumed that the atoms in our system can be treated as two-level systems. In general, though, the different Zeeman sublevels can give rise to interactions that mix angular momentum states, which in turn interact with different precise shapes of the dipole–dipole interaction [47, 48]. The study of these multilevel systems will be in the scope of future investigations. However, there are a number of situations in which a two-level approximation is a valid assumption on the system. For example, in atoms where the ground state is unique (angular momentum $J = 0$) —that can be achieved, again, in the case of alkaline-earth-metal atoms—the excited state has angular momentum $J' = 1$ and an effective two-level system can be realized by Zeeman splitting of the three degenerate states such that two of them are shifted out of resonance.

Acknowledgments

The authors would like to acknowledge Igor Lesanovsky for useful discussions. Also Michael R Hush and Deshui Yu are acknowledged for discussions in the very early stages of this work. This work was supported by the Royal Society and the Engineering and Physical Sciences Research Council (EPSRC) [grant number DH130145]. We are grateful for access to the University of Nottingham High Performance Computing Facility. This research has been supported by the EU-FET grant QuILMI 295293.

References

[1] Dicke R H 1954 *Phys. Rev.* **93** 99
[2] Lehmberg R H 1970 *Phys. Rev.* A **2** 883
[3] Agarwal G S 1970 *Phys. Rev.* A **2** 2038
[4] Bloch I, Dalibard J and Zwerger W 2008 *Rev. Mod. Phys.* **80** 885
[5] Röhlsberger R, Schlage K, Sahoo B, Couet S and Rüffer R 2010 *Science* **328** 1248
[6] Keaveney J, Sargsyan A, Krohn U, Hughes I G, Sarkisyan D and Adams C S 2012 *Phys. Rev. Lett.* **108** 173601
[7] Meir Z, Schwartz O, Shahmoon E, Oron D and Ozeri R 2014 *Phys. Rev. Lett* **113** 193002
[8] Pellegrino J, Bourgain R, Jennewein S, Sortais Y R P, Browaeys A, Jenkins S D and Ruostekoski J 2014 *Phys. Rev. Lett.* **113** 133602
[9] Kwong C C, Yang T, Pramod M S, Pandey K, Delande D, Pierrat R and Wilkowski D 2014 *Phys. Rev. Lett.* **113** 223601
[10] Kwong C C, Yang T, Delande D, Pierrat R and Wilkowski D 2015 *Phys. Rev. Lett.* **115** 223601
[11] Bromley S L *et al* 2016 *Nature Comm.* **7** 11039
[12] Jenkins S D, Ruostekoski J, Javanainen J, Bourgain R, Jennewein S, Sortais Y R P and Browaeys A 2016 .*Phys. Rev. Lett.* **116** 183601
[13] Jennewein S, Besbes M, Schilder N J, Jenkins S D, Sauvan C, Ruostekoski J, Greffet J-J, Sortais Y R P and Browaeys A 2016 *Phys. Rev. Lett.* **116** 233601
[14] Scully M O, Fry E S, Ooi C H R and Wódkiewicz K 2006 *Phys. Rev. Lett.* **96** 010501
[15] Goban A, Hung C-L, Hood J D, Yu S-P, Muniz J A, Painter O and Kimble H J 2015 *Phys. Rev. Lett.* **115** 063601
[16] Guerin W, Araújo M O and Kaiser R 2016 *Phys. Rev. Lett.* **116** 083601
[17] Ruostekoski J and Javanainen J 1997 *Phys. Rev.* A **55** 513
[18] Javanainen J, Ruostekoski J, Vestergaard B and Francis M R 1999 *Phys. Rev.* A **59** 649
[19] Fleischhauer M and Yelin S F 1999 *Phys. Rev.* A **59** 2427
[20] Scully M O 2009 *Phys. Rev. Lett.* **102** 143601
[21] Svidzinsky A A, Chang J-T and Scully M O 2010 *Phys. Rev.* A **81** 053821
[22] Bienaimé T, Piovella N and Kaiser R 2012 *Phys. Rev. Lett.* **108** 123602

[23] Bienaimé T, Bachelard R, Piovella N and Kaiser R 2013 *Fortschr. Phys.* **61** 377
[24] Olmos B, Yu D, Singh Y, Schreck F, Bongs K and Lesanovsky I 2013 *Phys. Rev. Lett.* **110** 143602
[25] Li Y, Evers J, Feng W and Zhu S-Y 2013 *Phys. Rev.* A **87** 053837
[26] Javanainen J, Ruostekoski J, Li Y and Yoo S-M 2014 *Phys. Rev. Lett.* **112** 113603
[27] Bettles R J, Gardiner S A and Adams C S 2015 *Phys. Rev.* A **92** 063822
[28] Javanainen J and Ruostekoski J 2016 *Opt. Express* **24** 993
[29] Lee M D, Jenkins S D and Ruostekoski J 2016 *Phys. Rev.* A **93** 063803
[30] Kuś M and Wódkiewicz K 1981 *Phys. Rev.* A **23** 853
[31] James D F V 1993 *Phys. Rev.* A **47** 1336
[32] Hettich C, Schmitt C, Zitzmann J, Kühn S, Gerhardt I and Sandoghdar V 2002 *Science* **298** 385
[33] Das S, Agarwal G S and Scully M O 2008 *Phys. Rev. Lett.* **101** 153601
[34] Wang D-W, Li Z-H, Zheng H and Zhu S-Y 2010 *Phys. Rev.* A **81** 043819
[35] Zoubi H and Ritsch H 2012 *Eur. Phys. J.* D **66** 292
[36] Ott J R, Wubs M, Lodahl P, Mortensen N A and Kaiser R 2013 *Phys. Rev.* A **87** 061801
[37] Scully M and Zubairy M (ed) 2008 *Quantum Optics* 6th edn (Cambridge: Cambridge University Press)
[38] Ates C, Olmos B, Garrahan J P and Lesanovsky I 2012 *Phys. Rev.* A **85** 043620
[39] Olmos B, Yu D and Lesanovsky I 2014 *Phys. Rev.* A **89** 023616
[40] Kimble H J and Mandel L 1976 *Phys. Rev.* A **13** 2123
[41] Diedrich F and Walther H 1987 *Phys. Rev. Lett.* **58** 203
[42] Gerber S, Rotter D, Slodička L, Eschner J, Carmichael H J and Blatt R 2009 *Phys. Rev. Lett.* **102** 183601
[43] Basché T, Moerner W E, Orrit M and Talon H 1992 *Phys. Rev. Lett.* **69** 1516
[44] Meiser D and Holland M J 2010 *Phys. Rev.* A **81** 063827
[45] Bhatti D, von Zanthier J and Agarwal G 2015 *Sci. Rep.* **5** 17335
[46] Auffves A, Gerace D, Portolan S, Drezet A and Frana Santos M 2011 *New J. Phys.* **13** 093020
[47] Kiffner M, Evers J and Keitel C H 2007 *Phys. Rev.* A **76** 013807
[48] Evers J, Kiffner M, Macovei M and Keitel C H 2006 *Phys. Rev.* A **73** 023804